

# WAXD and SEM Characterization of Two PAN Candidates as Carbon Fiber Precursors

ION PENCEA<sup>1\*</sup>, VIOLETA FLORINA ANGHELINA<sup>2</sup>, CATALIN EUGEN SFAT<sup>1</sup>, ION V. POPESCU<sup>2</sup>

<sup>1</sup>University Politehnica of Bucharest, Materials Science and Engineering Faculty, 313 Splaiul Independentei, 060042, Bucharest, Romania

<sup>2</sup>University "Valahia" of Targoviste, Materials Science and Engineering Faculty, 18-20 Unirii Blv., Targoviste, Romania

*Polyacrylonitrile (PAN) fibers are used on a large scale in textile industry but, some sorts of PAN fibers are valuable precursors for specific carbon fiber (CF) due to their best fitness to the purpose e.g. for high strength CF or for active CF. The application of PAN as precursors of CF is based on its specific structure and texture. Thus, the properties of PAN base CF strongly depend on PAN structure, texture and fiber morphology. In this respect, the paper addresses the modeling of PAN fiber structure and texture and, subsequently, estimation of structure and texture parameters based mainly on Wide Angle X-ray Diffraction (WAXD) technique but, on SEM and other data. The PAN fiber structure and texture parameters were calculated on the basis of classical X-ray diffraction theory applied to paracrystals. The preferred orientation parameters were calculated on a wide accepted model. The main structural parameter of PAN paracrystal  $d_{200}$ ,  $d_{200}^*$  and  $L_{200}$  and preferred orientation/texture parameters  $Z$ ,  $\langle \cos^2 u \rangle$ ,  $P(\cos^2 u)$  of the PAN fibers were determined. Based on WAXD data it was calculated the PAN fiber crystallinity. As it results from the paper the WAXD technique seems to be the best from the efficiency-cost point of view for PAN structure and preferred orientation characterization.*

**Keywords:** WAXD, SEM, structure, preferred orientation, polyacrylonitrile fibers

Polyacrylonitrile (PAN) fibers are extensively used in textile industry. Since, 1961 some sorts of PAN fibers are used as carbon fibers (CF) precursors [1 - 4].

The PAN base CF are over 85% of world CF production due to their relative low cost and the ability to be adapted to the designed CF characteristics. Thus, about all high strength CF for aircraft applications have PAN precursors. It has already been established that PAN fibers not only serve as the most suitable precursor, but also the properties of the ultimate carbon fibers depend largely on the characteristics of the precursor [5-9]

In the last years, the active CF (ACF) became an attractive solution for specific environmental applications due to their high performance as adsorbents and absorbents [10]. The ACF has the advantage of a controlled porosity comparing with biomass or coal active carbon [11, 12].

As it is easy to understand, the technologies for CF and ACF based on PAN precursors are matters of know-how, thus there is a small amount of published information on these subjects. Besides, if one used a new PAN precursor for CF or ACF then the technological parameters have to be adjusted to the new precursor otherwise he risks getting worse CF or ACF. This was the problem encountered by a research team in charge with establishing a production technology for PAN base CF used for reinforcing advanced composite. The team used various techniques for PAN fiber characterization and for resulting CF as: optical microscopy, SEM, tensile test and two **WAXD** techniques i.e. diffractometry and Debye-Scherrer camera. Each investigation technique had provided useful information but WAXD have provided critical data that help us to establish and control some critical parameters of the PAN CF manufacture in the manner of published data [13, 14]. Some of significant WAXD data are the issue of this paper.

## PAN fiber structure and preferred orientation model PAN fiber chemistry

The chemical formula of PAN is:



where  $n$  is the number monomers known as the degree of polymerization.

The most industrial PAN fibers are of copolymer nature containing 2-10% comonomers, as methyl acrylate or methyl methacrylate. PAN also contains a small quantity of catalytic comonomers, for stabilizing reactions at low temperatures as itaconic acid, especially. The compositions of the investigated PAN fibers are specified in table 1.

**Table 1**

CHEMICAL COMPOSITIONS OF THE INVESTIGATED PAN FIBERS

Sample code	PAN Sv 41	PAN Sv 61
Acrylonitrile	94.6	95
Methyl Acrylate	4.0	5.0
Itaconic Acid	1.4	1.0

Di-methyl formamide or sodium tri-cyanide are the main organic solvents used in the wet or dry spinning process of PAN. The most PAN precursors of CF are produced as yarn of 3000 ÷ 12000 fibers by wet or dry spinning technology. The commercial PAN fibers are of 6 ÷ 12  $\mu\text{m}$  in diameter but most of the grades are of 8  $\mu\text{m}$  in diameter. The spinning process produces a high preferred orientation of the macromolecule chains parallel to the fiber axis [15, 16].

*Paracrystalline model of PAN fiber structure*

\* email: ini.pencea@yahoo.com

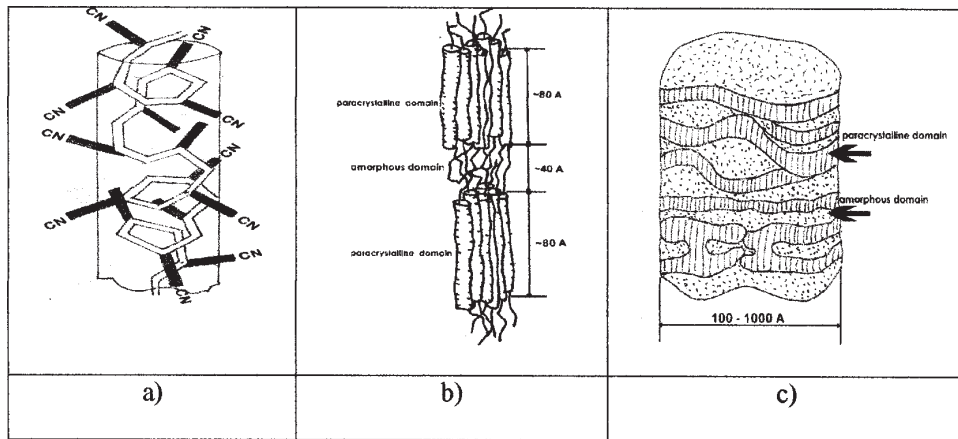


Fig. 1. Schematic illustration of the PAN structural levels: a) fibril; b) macromolecular orientation; c) macromolecule helical structure

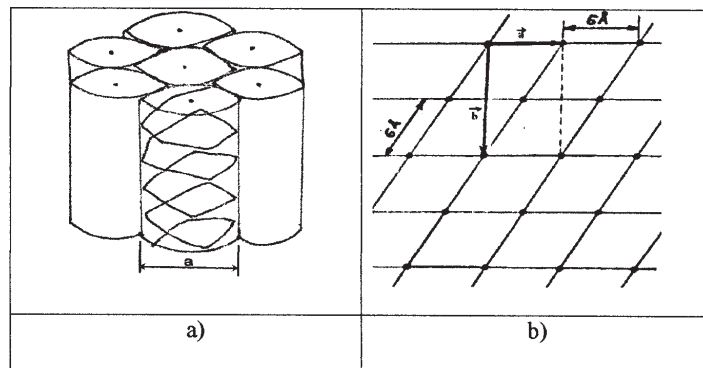


Fig. 2. The PAN paracrystalline structural model; a) close packed macromolecule; b) 2D lattice associated to the paracrystalline structure

The most accepted molecular model of PAN fiber is schematically shown in figure 1.(a÷c) [3, 5, 6, 15]. The structural model of PAN fiber precursor could be structured on three levels: helical macromolecule (fig. 1.a), *paracrystal* consisting of close packed macromolecule of cylindrical shape (fig. 1.b), fibril consisting of paracrystalline domains (fig. 1.c).

The rod-shape (“wand”) macromolecule has a significant stiffness due to van der Waals bonds between the comonomer on the consecutive coil of helices (fig. 1.a).

The aligned macromolecules bond each other by atomic links and became entrapped each-other into a bundle of close-packed macromolecules that form a so called paracrystal having two-dimensional order in the fibril cross-section of hexagonal type (fig 2. a, b). The most convenient unit cell of PAN paracrystal is an orthogonal one with **a** parameter equal to macromolecule diameter ranging in 0,5÷0,6 nm.

In the frame of orthogonal symmetry the **b** axis is perpendicular to **a** axis and is about  $1.73/a$  in length (fig. 2.b). The **c** axis is conventionally normal to (**a**, **b**) plane and has an arbitrary length.

It makes sense to consider that at the end of a paracrystal the packed order diminishes due to different macromolecule length and other factors. Thus, the fibril consists of interlinked ordered and disordered domains.

#### Preferred orientation of PAN precursor

The PAN fiber paracrystals align with **c** axes quite parallel to the fiber axis while **a** axis orientations are uniformly distributed in the fiber cross-section [11, 12, 15, 16, 17]. The preferred orientation degree of a PAN precursor is a key clue for CF production and is a matter of know-how. Thus, each producer has to establish on his own means

this ratio and other parameters of PAN precursor for a specific purpose.

According to the PAN paracrystal nature the orientation of a macromolecule rod related to the fiber axis defines the orientation of the crystal it will be part of. The distribution function  $T(u)$  of **c** vectors related to the director vector (fiber axis) depends only of **u** azimuth angle because the PAN fiber has cylindrical symmetry. In this case, the most used function for preferred orientation estimation of polymers is the Herman orientation function  $f$  [5, 15, 18, 19, 20].

$$f = (3\cos^2(u) - 1)/2 \quad (2)$$

where **u** is the angle between the fiber and macromolecule axis e.g. **c** axis of paracrystal [13,19, 20]. Though, there are other preferred orientation parameters considered more convenient for preferred order estimation as:  $Z$ ,  $\langle \cos^2(u) \rangle$ ,  $P_2$  etc [21, 22] defined as:  $Z$  is the meridian angular half width of (200) WAXS peak.

$$\langle \cos^2(u) \rangle = \int_0^{2\pi} \int_0^{\pi} \cos^2(u) \cdot T(u,v) \cdot \sin u \cdot du dv \quad (3)$$

where **u**, **v** are the spherical coordinate angles.

$$P_2 = \frac{1}{2} \cdot (3\langle \cos^2(u) \rangle - 1) \quad (4)$$

where  $P_2$  is in fact the average of  $f(u)$ .

The form of parameter  $P_2$  is considered as follows: a perfectly ordered fiber has a  $P_2$  parameter that is equal to the unit and the isotropic material has a null one e.g.  $P_2 \in [0,1]$ .

The X rays diffraction methods are usually used to determine these parameters [13, 14, 22]. Therefore, the number of the normal on the (hkl) planes that cross the reference sphere in the solid angle element is proportional to the intensity of X radiation diffracted to a correlated angle ( $\phi, \psi$ ) with  $\phi = u + \pi/2$  and  $\psi = v$  e.g.  $I(\phi, \psi)$ . Thus,  $\langle \cos^2 \phi \rangle = \langle \cos^2 u \rangle$  and can be evaluated as follows:

$$\langle \cos^2 \phi \rangle = \frac{\int_0^{2\pi} \int_0^{\pi/2} I(\phi, \Psi) \cos^2 \phi \cdot \sin \phi \cdot d\phi d\Psi}{\int_0^{2\pi} \int_0^{\pi/2} I(\phi, \Psi) \sin \phi \cdot d\phi d\Psi} \quad (5)$$

Taking into account the cylindrical symmetry of  $I(\phi, \psi)$  the integral over  $\psi$  in rel.(5) can be written as:

$$I(\phi) = \int_0^{2\pi} I(\phi, \Psi) d\Psi \quad (6)$$

and rel.(5) becomes:

$$\langle \cos^2 \phi \rangle = \frac{\int_0^{\pi/2} I(\phi) \cos^2 \phi \cdot \sin \phi \cdot d\phi}{\int_0^{\pi/2} I(\phi) \sin \phi \cdot d\phi} \quad (7)$$

In the above context,  $I(\phi)$  represents the distribution function of the normals in polar coordinates. The distribution function of the normals is proportional to the integral intensity diffracted by the associated (hkl) planes.

### Experimental part

The paper addresses two Romanian PAN precursor sorts e.g. PAN Sv 41, PAN Sv 61. Also, the paper addresses mainly WAXD investigations of PAN precursor and subsidiary the SEM and optical microscopically investigations. The WAXD investigations were done with a DRON 3 diffractometer for structural parameter estimation while for preferred parameter estimation was used a Debye-Scherrer camera, with the diameter  $\phi = 57.3$  mm and Ni filtered  $\text{CuK}_\alpha$  radiation. The diffractometric data were corrected according to classical procedure [23, 24].

The distances between (hk0) planes were calculated on the base of well-known Bragg relation :

$$2 \cdot d \cdot \sin(\theta) = n\lambda \quad (8)$$

where

$d$  is the inter-planar distance;

$\theta$  - the Bragg angle;  $\lambda$  is the wavelength of X-ray beam.

The crystallite size ( $L_{(200)}$ ) was calculated from the Scherrer formula:

$$L_{(200)} = K \cdot \lambda / [B \cdot \cos(\theta)] \quad (9)$$

where:

$K = 0.89$  is a constant;

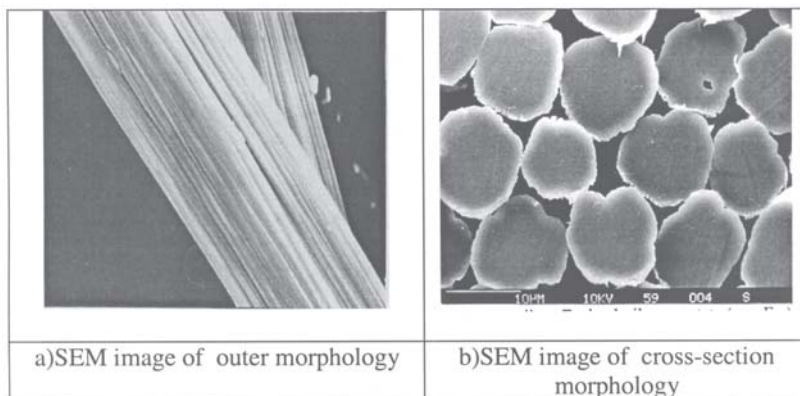


Fig. 4. Significant lateral (a) and cross-section (b) morphologies of the PAN Sv 41 precursor

$\lambda$  - the wavelength of the diffracted X-ray,  $B$  is the full width at half the maximum intensity (FWHM) of the (200) peak.

The crystallinity ( $X_c$ ) of fibers is measured by Hinrichen's method [25, 26]:

$$X_c = [I_c / (I_c + I_a)] \cdot 100\% \quad (10)$$

where

$I_c$  is the integral intensity of crystalline fraction which is the area under the diffraction peaks and background curve;

$I_a$  - the intensity scattered by the amorphous fraction which is the area of the diffractogram outside the peaks.

The uncertainties of crystalline and preferred orientation measurements are complicated to estimate thereof the crystallinity and preferred orientation of the candidate PAN precursors should be interpreted only by comparison with the reference materials (RM).

The SEM images were taken with a TESLA BS 350 microscope while optical investigation was performed with a Karl Zeiss one.

### Results and discussion

Besides the chemical composition of PAN fibers their morphology (diameter, cylindrical shape, surface smoothness, the density of surface defects as wide pores, notches, solid particles etc) is critical for high strength carbon fiber manufacture. Usually, the morphology of PAN fibers is investigated by scanning electron microscopy (SEM) and seldom by optical microscopy using non-polarized and/or polarized light (fig. 3).

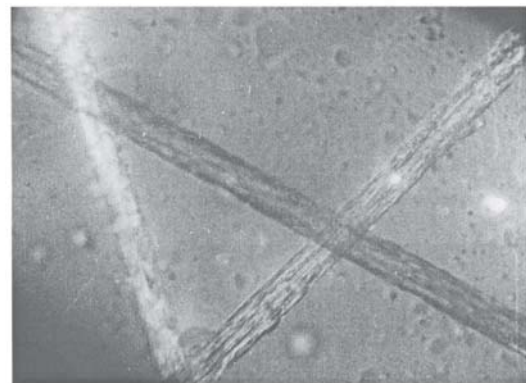


Fig. 3. Optical image of PAN Sv 41 fibers, polarized light (x200)

The main morphological characteristic of the lateral surface of PAN fibers is the fibrile pattern as it results from figure 3, but obviously from figure 4. This pattern is produced by the spinning and stretching processes during PAN fiber production but due to PAN macromolecular nature. The PAN fiber morphology (lateral surface aspects, cross-section pattern, average diameter, porosity), (fig. 5 and fig. 6), is responsible for CF mechanical strength ( $\sigma$ ),

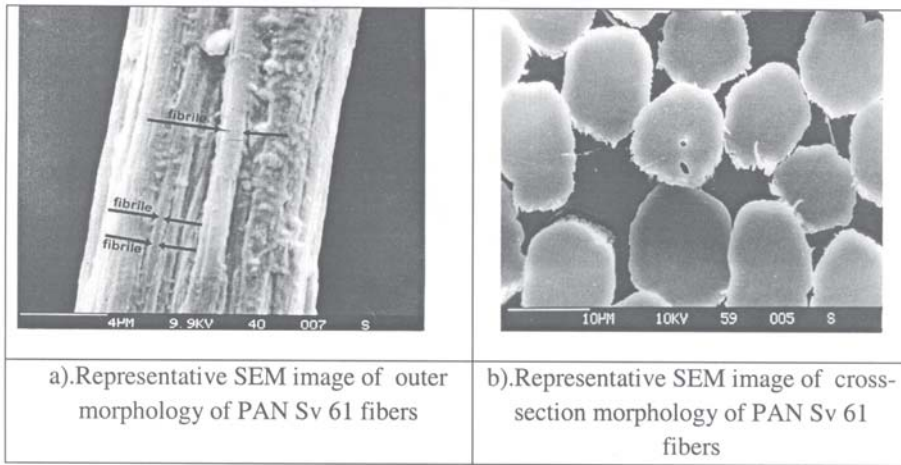


Fig. 5. Significant lateral(a) and cross-section (b)morphologies of the PAN Sv 61 precursor

flexural failure etc. The morphology of PAN Sv 61 is quite similar to the morphology of PAN Sv 41, (fig. 5 and fig. 6).

SEM investigations showed that PAN Sv 41 could be used as precursors for medium or even high strength CF while PAN Sv 61 could be used for filler CF or better for ACF. It is to underline that a PAN precursor for high-strength CF must have a cylindrical morphology with smooth surface without porosity.

The samples for WAXD investigation consists of aligned PAN bundles of the same volume. The bundles were aligned parallel to the diffractometer goniometer axis so that the diffracted intensities to be comparable from the irradiated volume point of view. The diffractogram given by the PAN Sv 41 and PAN Sv 61 samples are quite similar and comply to the reported patterns [15, 27, 28] as it results from figure 6. a), b).

The peak positions in figure 6 a), b) were used to estimate the (200) ( $d_{200}$ ) and (310) ( $d_{310}$ ) interplanar distances while their FWHM for the apparent average diameters of the PAN paracrystals in the  $\langle 200 \rangle$  and  $\langle 310 \rangle$  directions ( $L_{200}$  and  $L_{310}$ , respectively). The integral intensities of the (200) and (310) lines were considered as  $I_c$ . The uncertainties of the measurand given in table 2 were calculated on the base of error propagation low i.e. in

the hypothesis that the influence factors are of random nature and comply to normal density distribution [29]. The extended uncertainty factor was taken as 2 e.g. the significant degree is 0,05 or the degree of confidence is 95%.

The structural parameters of PAN samples are consistent with those published by different authors [3, 13, 24, 25] and with the data obtained by our laboratory on Courtella, Beslon or Toray PAN fiber. The extended uncertainties associated to interplanar distances are quite reasonable e.g. less than 2% while those associated to average diameters and crystallinity range from 15 to 20%. On the other hand, the way of defining  $L$  and  $X_c$  prone to bigger uncertainties. Nevertheless, there is further little to be done to improve the exactness of WAXD method because the influence factors of the WAXD technique applied to PAN fiber are difficult to be kept under control as: fiber alignment, fiber tensile, bundle volume, fiber density etc.

Unfortunately, the WAXD data are insufficient for technologists thus the PAN fiber preferred orientation was investigated by Debye-Scherrer technique. The geometry of the Debye-Scherrer experiment is given in figure 7.

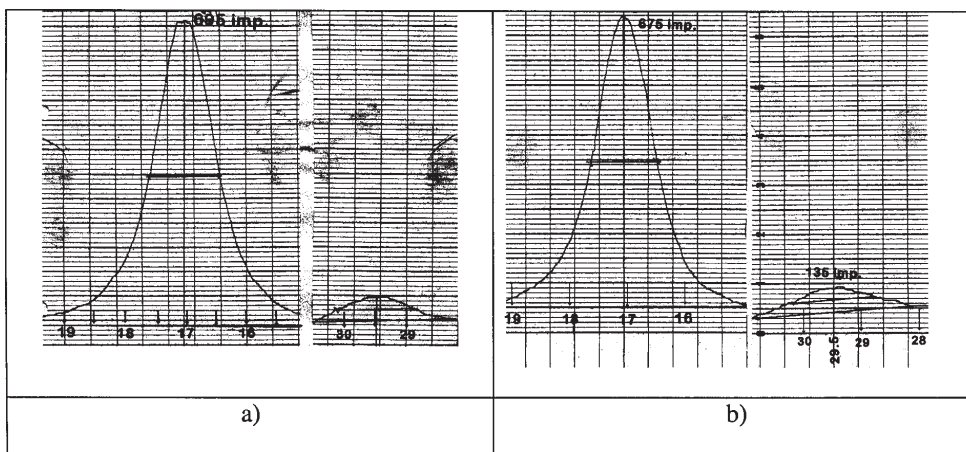


Fig. 6. Diffractograms of CF PAN precursors: a) PAN Sv 41, b) PAN Sv 61

sample	$d_{200}$	$U_d$ (95%)	$L_{200}$ (nm)	$U_L$ (95%)	$d_{310}$	$U_d$ (95%)	$L_{310}$ (nm)	$U_L$ (95%)	$X_c$	$U_x$ (95%)
PAN Sv 41	5,18	0,09	67	11	3,03	0,06	66	11	0,52	0,08
PAN Sv 61	5,40	0,10	80	16	3,06	0,06	41	8	0,49	0,08

Table 2  
STRUCTURAL PARAMETERS OF PAN Sv 41 AND OF PAN Sv 61 ESTIMATED BY WAXS

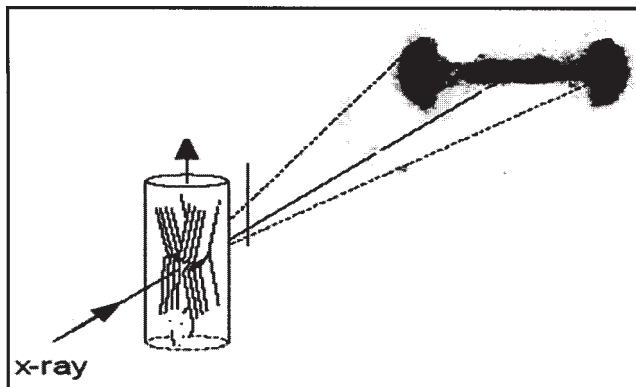


Fig. 7. The geometry of the Debye-Scherrer experiments

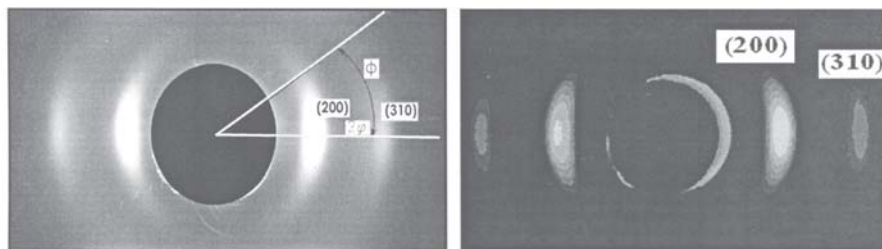


Fig.8. Debyegrams for PAN Sv 41 and PAN Sv 61

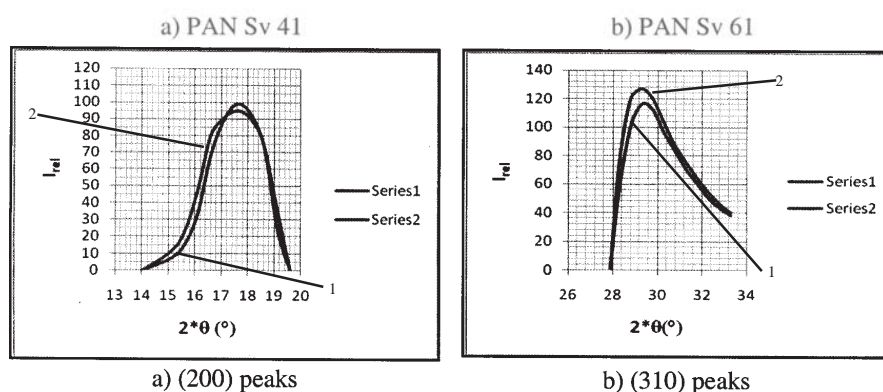


Fig.9. Densitometric curves for PAN-Sv 41(1) and PAN Sv 61(2)

The diameter of the camera is  $\phi = 57.3\text{mm}$ . The  $\text{CuK}_{\alpha}$  X-ray beam was Ni filtered. The PAN fiber bundle was aligned parallel to the camera axis. Two representative Debyeagram taken on PAN Sv 41 and PAN Sv 61 samples are shown in fig. 8 a),b).

The WAXS images of the PAN Sv 41 and of PAN Sv 61 sample (fig 8 a), b) show that these fibers have similar preferred orientation.

The Debyegrams show net (200) and (310) peaks. The densitometry curves of the diffraction maximum peaks (200) and (310) are shown in fig.9 a),b). As it results from figure 9.a, the positions of the main maximum peak (200) of PAN-Sv 41 and PAN Sv 61 fibers are closer and the FWHMs are also very similar.

Figure 9.b shows that (310) line profiles are asymmetrical and have the same shape for PAN Sv 41 and PAN Sv 61 fibers. The structural parameters estimated based on densitometric curves are given in table 3. The

extended uncertainties with 95% degree of confidence show that the structural data obtained by Debye-Scherrer technique are consistent with the diffractometric ones.

The structural data in table 3 are significantly different from data in table 2 especially for average diameters. These differences are caused by multiple factors as different technique for X-ray beam collimation, filtration, detection: different irradiation time etc. It is quite a matter of evidence, that the Debye-Scherrer technique could provide structural data as  $d_{200}$ ,  $d_{310}$ ,  $L_{200}$  and  $L_{310}$  but at lower quality than WAXD technique. On the other hand, Debye-Scherrer technique is the best for PAN fiber preferred orientation investigation as figure 8 shows.

In order to estimate the orientation parameter Z, there were photogrametred the (200) arcs of the Debyegrams in figure 8 along the meridian and there were obtained the profiles  $I(\phi)$  for both samples. The HWHM of the

sample	$d_{200}$ (Å)	$U_d$ (95%)	$L_{200}$ (nm)	$U_L$ (95%)	$d_{310}$ (Å)	$U_d$ (95%)	$L_{310}$ (nm)	$U_L$ (95%)
PAN Sv 41	5.14	0.09	3.08	0.041	3.03	0.06	3.01	0.043
PAN Sv 61	5.24	0.09	3.06	0.043	3.04	0.06	3.06	0.044

Table 3  
STRUCTURAL PARAMETERS FOR  
PAN Sv 41 AND PAN Sv 61  
PRECURSORS

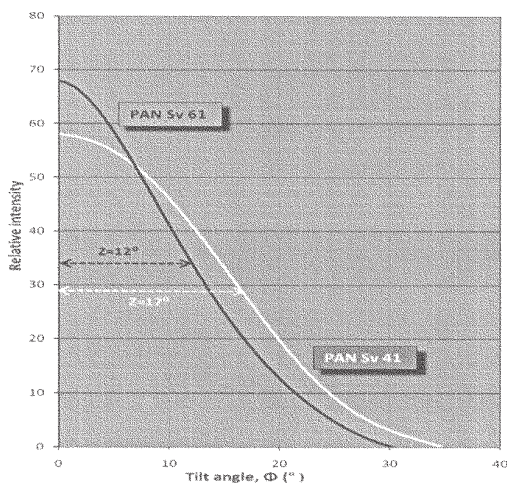


Fig.10. Z parameters of PAN Sv 41 and PAN Sv 61

densitometric curves e.g. Z parameters of the samples are given in table 4.

Table 4

PREFERRED ORIENTATION PARAMETERS OF THE PAN SAMPLES

Fiber type	Z	$\langle \cos^2\phi \rangle$	$P_2(\langle \cos^2\phi \rangle)$
PAN Sv 41	17°	0,83	0,75
PAN Sv 61	12°	0,85	0,77

The  $\langle \cos^2\phi \rangle$  has been calculated using the graphical integration method to estimate the nominator and denominator in rel.(7). Once the  $\langle \cos^2\phi \rangle$  is estimated then  $P_2$  is quite easy to calculate. Unfortunately, the uncertainty of the  $\langle \cos^2\phi \rangle$  is very difficult to estimate or even impossible. Thus, the quality of the preferred orientation parameters  $\langle \cos^2\phi \rangle$  and also of  $P_2$  remains doubtfully. Anyhow, by the authors knowledge, in the literature there is no specification about the quality of the structural and preferred orientation parameters of PAN fibers. The Z parameters of both samples seem to be significantly different while  $\langle \cos^2\phi \rangle$ s and  $P_2$ s seem to be quite equal if we take into account at least 10% relative uncertainties associated to  $\langle \cos^2\phi \rangle$  and  $P_2$ .

From Z value point of view the PAN Sv 41 sample is similar to the consecrated PAN precursors mentioned above while PAN Sv 61 is less preferred oriented. But, based on the values of  $\langle \cos^2\phi \rangle$ s and  $P_2$ s one can conclude that both PAN precursors fulfill the preferred orientation requirements.

## Conclusions

The paper shows why the SEM and WAXD techniques (diffractometry, Debye-Scherrer) are of great interest for PAN fiber testing.e.g.underlines the effectiveness of the classical WAXD and SEM technique for the PAN carbon fiber manufacture.

The paper argues that diffractometry is better fitted for PAN fiber structure characterization while Debye-Scherrer technique for preferred orientation characterization. Also, the paper proves the role of uncertainty in results quality assurance.

The WAXD results prove that the structure and texture of of PAN Sv 41 and PAN Sv 61 are very similar to the ones that had been described in [27] and in [28] for the same type of fiber.

The WAXD and SEM results made the main part of inference if a PAN fiber is proper to be considered as precursor for a specific type of carbon fiber. In this sense, the PAN Sv 41 and PAN Sv 61 are most fitted for medium strength carbon fiber. Also, they could be used as ACF precursor but from economical point of view this is not recommended.

The quality of WAXD results could be improved if there will be developed special equipment provided with texture goniometer and a hemispherical PPD detector but this means at least one thousand more than those for a routine Debye-Scherrer camera. Besides, the expected quality enhancement will not exceed 10 times which is unbearable.

## References

- SHINDO, A., Rep. Govn. Md. Res. Osaka, 1961, p. 317
- JOHNSON, W., PHILLIPS, L., WATT, W., Brit. Pat., 1,110,1964, p 791
- FITZER, E., Carbon, **27**, 1989, p. 621
- ESLAMI FARSANI, R., SHOKUH FAR, A., SEDGHI, A., Rep. on Conversion of Modified Commercial Polyacrylonitrile Fibers to Carbon Fibers, World Academy of Science, Engineering and Technology, **35**, 2007
- CHAIR, S. S., BAHL O.P., MATHUR, R. B., Fiber Sci. Technology, **15**, 1981, p. 153
- MATHUR, R. B., BAHL, O. P., KUNDRA, K. D., J of Mat. Sci. Letters, **5**, 1986, p. 757
- ZUSSMAN, E., CHEN, X., DING, W., CALABRI, L., DIKIN, D.A., QUINTANA, J.P., RUOFF R.S., Carbon, **43**, 2005, p. 2175
- MELJIE, Y., CHENGGUO, W., YUJUN, B., YANXIANG, W., YONG, X., Polymer Bull. **57**, 2006, p. 757
- VASILIU, F., PENCEA, I., Popov, A.M., Rev. Phys. Studies and Researches, **43**, 3-4, 1991, p 135
- VASILIU, F., PENCEA, I., Rev. Phys. Studies and Researches, **43**, 3-4, 1991, p 156
- KONOVALOVA, L. YA., NEGODYAEVA, G. S., KUMOK, I. L., TIKHOMIROVA, M. V., DORENSKII, A. L., IOVLEVA, M. M., AZAROVA, M. T. "Carbon And Other Heat Resistant Fibers, Composite Materials, And Use Of These In National Economy" Publisher Springer New York, ISSN0015-0541 (Print) p. 1573-8493, (Online) Issue Volume 23, Number 3 / May, 1992, DOI10.1007/BF00545862, p.193
- YOSHINOBU, K., SHIRO, I., HIROSHI, F., ISAO M., Fuel, **63**, 12, 1984, p. 1738
- LIU, X.D., RULAND, W., Macromolecules, **26**, 1993, p. 3030
- BELENKOV, E. A., Russian Journal of Applied Chemistry, **72**, 9, 1999, p. 1612
- FITZER, E., FROHS, W., HEINE, M., Carbon **24**, 1986, p. 387
- BUMSUK JUNGA, JOON KI YOONA, BOKYUNG KIMA, HEE-WOO RHEEB, Journal of Membrane Science, 246, 2005, p. 67
- LIANJIANG TAN, HUIFANG CHEN, DING PAN, NING PAN, European Polymer Journal **45**, 2009, p.1617
- PICK, M., LOVELL, R., WINDLE, A. H., Polymer, **21**, Issue 9, 1980, p.1017
- \*\*\*, www.polymer.kth.se/grundutbildning/.../Chapter%207.pdf]
- PARIS, O., LOIDL, D., PETERLIK, H., Carbon, **40**, Issue 4, 2002, p. 551
- ZHI-XIAN X, JING X, LIANG-HUA X, YONG-QIANG D, LI-WEI AND RI-GUANG J, Polymer(Korea), **32**, No. 2, 2008, p. 150
- PENCEA, I., Elements of applied structural analysis, Ed. PrintTech, Bucharest, 2001, p.
- PENCEA, I., Basics of structural analysis, Ed. Print Tech, Bucharest, 2001, p.
- DRAMBEI, P., CIOCOIU, M., DRAMBEI, C., CRAUS, M.L., Mat. Plast. **46**, no. 3, 2009, p. 310
- HINRICHSSEN, G., J Polym. Sci. **38**, 1972, p. 303
- LIPATOV, I. S., et.all, Rentgenograficeschie metodi izucenia polimernish sistem, Ed. Nauka Duma.jkasjkb, 1982, p.
- CHARI S. S., BAHL O.P., Fiber. Sci. Tech. **15**, 1981, p. 153.
- MATHUR, R. B., BAHL, O.P și alții, Fib. Sci. Technol. no. 21, 1984, p. 223
- \*\*\*\*, SR EN 13005, 2005, p.74

Manuscript received: 2.03.2010